VOLUME 34 NUMBER 9
ACCOUNTS of CHEMICAL RESEARCH®
SEPTEMBER 2001

Understanding the Phase-Dependent Reactivity of Chlorine Dioxide Using Resonance Raman Spectroscopy

PHILIP J. REID*
Department of Chemistry, Box 351700, University of Washington, Seattle, Washington 98195

Received April 4, 2001

ABSTRACT
Progress in understanding the phase-dependent reactivity of chlorine dioxide (OClO) is outlined. Resonance Raman intensity analysis studies of gaseous and solution-phase OClO are presented which demonstrate that the optically prepared excited state undergoes significant modification in solution. In addition, time-resolved resonance Raman studies are presented which demonstrate that geminate recombination of the primary photoproducts, resulting in the re-formation of ground-state OClO, dominates the photochemical reaction dynamics in solution. The current picture of aqueous OClO photochemistry derived from these studies is discussed, and future directions of investigation are outlined.

Introduction

The chemistry of halooxides has been of interest for the past two centuries.[1] However, it was the observation of seasonal stratospheric ozone loss over Antarctica that generated a renaissance in interest regarding the reactivity of these compounds.[2] Specifically, the suggestion that anthropogenic sources of chlorine were responsible for the transport and subsequent production of atomic chlorine in the stratosphere provided the impetus for studies designed to understand the halogen-based chemistry that results in ozone loss.[3,4] The culmination of this work has led to the identification of species that participate in stratospheric ozone depletion. Numerous chemical and/or photochemical processes have been identified as being important in the uptake and release of atomic chlorine (Cl), the dominant species responsible for ozone depletion for chlorine-mediated chemistry. A simplified schematic of these processes is presented in Figure 1.[5] The figure demonstrates that in addition to Cl, also of importance are reservoir species that do not directly participate in catalytic ozone depletion but can release reactive species through some chemical or photochemical transformation. For example, the photoexcitation of chlorine nitrate ($ClONO_2$) or hypochloric acid (HOCl) results in the production of Cl, which is highly reactive toward ozone. Removal of atomic chlorine is achieved predominately through hydrogen abstraction from hydrocarbons (dominated by methane as indicated in the figure). The abundance of ozone relative to hydrocarbons in the stratosphere is such that each chlorine atom can remove as many as 10^6 ozone molecules before removal.[5]

Modeling stratospheric ozone loss requires accurate knowledge of the rates and product formation efficiencies of reactions involving halogen-containing compounds. In addition, it has been recognized that the rates and efficiencies for these processes vary as a function of phase.[3,6,7] The presence of condensed environments such as aerosols or polar stratospheric clouds (PSCs) of type I (nitric acid trihydrates) and type II (water/ice) can serve to promote chemistry which differs significantly from that in the gas phase. A current challenge in atmospheric chemistry is not only to determine the extent to which a given reaction changes as a function of environment, but also to understand the fundamental details behind this behavior. Such knowledge will significantly increase our prognosticative abilities regarding stratospheric chemistry.

Our laboratory is interested in understanding the phase-dependent photochemical reactivity of halooxides. The chemistry of these compounds demonstrates remark-

Philip J. Reid was born on July 22, 1964, in Bremerton, WA. He has attended the University of Puget Sound (B.S.), the University of California, Berkeley (Ph.D. under the supervision of Richard Mathies), and the University of Minnesota (postdoc under the supervision of Paul Barbara). He joined the Department of Chemistry at the University of Washington, Seattle, in 1995 as an Assistant Professor and was promoted to his current position of Associate Professor in 2000. In addition to environmental photochemistry in homogeneous and heterogeneous environments, Prof. Reid is interested in biophysical chemistry, photochemistry in supercritical fluids, and the characterization of nonlinear optical materials using spectroscopic techniques.

* E-mail: preid@chem.washington.edu.

10.1021/ar010064u CCC: $20.00
Published on Web 07/12/2001

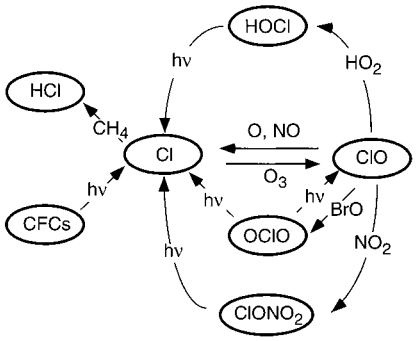

FIGURE 1. Simplified schematic of the reactive chlorine cycle. Adapted from *The Chemistry of Atmospheres*.[5]

able environmental dependence, with chlorine dioxide (OClO) serving as an excellent example of this reaction class.[8,9] Two photochemical pathways are available to OClO following photoexcitation (Figure 1): dissociation to form ClO and O, or Cl and O_2. What is remarkable about this photochemistry is that the quantum yield for Cl production (Φ_{Cl}) is extremely phase dependent. For example, Φ_{Cl} is only ~0.04 in the gas phase but increases to near unity in low-temperature matrixes.[10−13] The chemistry in solution is intermediate between these two limits, with $\Phi_{Cl} = 0.1$ in water.[14] The environmental impact of OClO is dependent on its ability to produce Cl, which apparently increases significantly in condensed environments. Studies of OClO on model PSCs suggest that equilibrium concentrations on such surfaces will be modest, thereby limiting the contribution of OClO to stratospheric ozone depletion.[15,16] However, this compound does serve as an excellent case in which to investigate solvent-dependent photochemical reactivity in an environmental context. In our work, we employ a multidimensional experimental approach that utilizes three distinct spectroscopic techniques: resonance Raman intensity analysis (RRIA), time-resolved resonance Raman (TRRR), and femtosecond pump−probe (FPP). The synergistic application of these techniques allows for the study of photochemical reactivity from the initial excited-state evolution to the appearance and relaxation of the ground-state products. In this Account, we summarize the major findings from our recent studies and outline how these results have contributed to our current understanding of OClO photochemistry. Although our focus here is on OClO, it should be kept in mind that the questions addressed here are common to many reactions of environmental importance. As such, this work represents not only an attempt to understand OClO photochemistry but also an attempt to develop an experimental methodology that is applicable to a wide range of environmental processes.

The Excited-State Reaction Dynamics of OClO

Background. Numerous spectroscopic studies of gaseous OClO have been performed, largely motivated by the fact that this compound is a relatively stable open-shell system. Early work focused on the electronic absorption spectrum of OClO, and most notably the band centered at ~360 nm assigned as the $^2B_1$ (ground) to $^2A_2$ (excited) transition.[8] This transition exhibits significant vibronic structure consistent with the predissociative nature of the $^2A_2$ surface. The first detailed study of this transition was performed by Coon, who noted the anomalous intensity for overtone transitions involving asymmetric stretch, demonstrating that the ground and excited potential energy surfaces differ substantially along this coordinate.[17] It was proposed that the origin of this intensity was the presence of a double-minimum potential along the asymmetric-stretch coordinate in the excited state. Support for this hypothesis was later provided by an elegant gas-phase absorption study of rotationally cold OClO performed by Richard and Vaida.[18,19] In this study, the relative intensities of transitions involving the asymmetric stretch were accurately reproduced using the double-minimum model. However, alternatives to this model have been proposed. In particular, Brand and co-workers suggested that anharmonic coupling between the symmetric- and asymmetric-stretch coordinates could provide for the anomalous intensity.[20] Ab initio results reported by Peterson and Werner were consistent with a single minimum along the asymmetric-stretch coordinate in support of the anharmonic-coupling model.[21,22] Consensus as to the nature of the $^2A_2$ surface along the asymmetric-stretch coordinate has not been achieved; however, both models predict that substantial evolution along the asymmetric-stretch coordinate occurs following photoexcitation. This prediction raises the question, does evolution along the asymmetric-stretch coordinate indeed occur upon photoexcitation? If so, is this evolution phase dependent?

We have used absolute resonance Raman intensity analysis (RRIA) to study the excited-state relaxation dynamics of OClO in the gas and condensed phases. Numerous reviews are available which discuss the details of this technique; therefore, only a brief description is presented here.[23,24] In RRIA, the variation in the absolute Raman scattering cross sections as a function of the excitation wavelength is measured, and this information is used in conjunction with the electronic absorption spectrum to develop a model of the optically prepared excited state. This model then defines the structural evolution that occurs following photoexcitation. The connection between excited-state structural evolution and resonance Raman/absorption intensities was illustrated by the time-dependent formalism of Heller and coworkers.[25,26] In this formalism, the equations that link the Raman (σ_R) and absorption (σ_A) cross sections to excited-state structural evolution are as follows:

$$\sigma_R(E_l) \propto \left|\int_0^\infty \langle f|i(t)\rangle \exp[i(E_l + E_i)t/\hbar]D(t)\,dt\right|^2$$

$$\sigma_A(E_l) \propto \int_{-\infty}^{\infty} \langle i|i(t)\rangle \exp[i(E_l + E_i)t/\hbar]D(t)\,dt$$

In the above expressions, E_l is the energy of the incident field, E_i is the energy of the vibration of interest, and $D(t)$ is a function included to reflect vibronic dephasing. The most important components of the above expressions are the time correlators $\langle f|i(t)\rangle$ and $\langle i|i(t)\rangle$. Resonance Raman intensities are dependent on $\langle f|i(t)\rangle$, which represents the

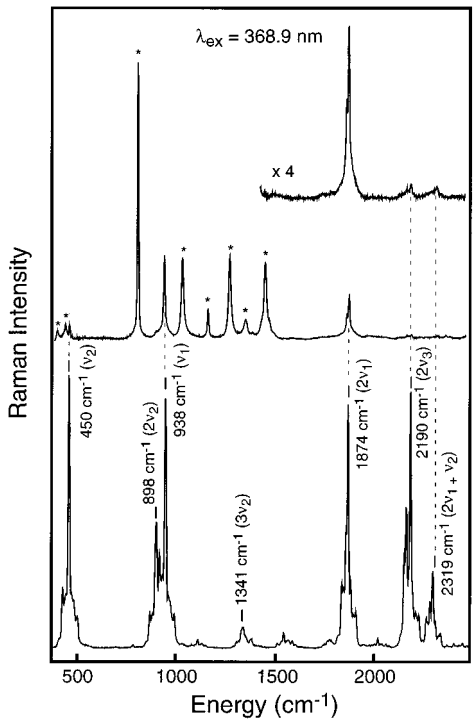

FIGURE 2. Resonance Raman spectra of gaseous chorine dioxide (OClO) and OClO dissolved in cyclohexane. The bottom spectrum is that of gaseous OClO. Transitions corresponding to the symmetric stretch (ν_1), bend (ν_2), and asymmetric stretch (ν_3) are indicated. The middle spectrum is that of OClO dissolved in cyclohexane. Peaks marked with an asterisk are due to the solvent. An expanded view of the overtone region is provided by the top spectrum. Note the reduction in asymmetric-stretch overtone intensity in cyclohexane relative to that in the gas phase.

overlap of the final state in the scattering process with the initial state propagating under the influence of the excited-state Hamiltonian. In analogous fashion, the absorption intensity is related to $\langle i|i(t)\rangle$, corresponding to the time-dependent overlap of the initial ground state with the propagating state. One can envision these terms as being time-dependent Franck−Condon (FC) factors that become finite due to differences in geometry between the ground and excited states. Therefore, the observation of resonance Raman intensity is evidence that excited-state structural evolution occurs along the corresponding vibrational coordinate. Since the resonance Raman and absorption cross sections both depend on $|i(t)\rangle$, these spectroscopies can be used in tandem to develop a self-consistent, mode-specific description of the excited-state potential energy surface. Furthermore, this analysis can be performed in a variety of environments, providing the opportunity to examine the dependence of excited-state structural evolution on environment.

RRIA of OClO in the Gas and Condensed Phases. Figure 2 presents the resonance Raman spectrum of gaseous OClO obtained with 368.9-nm excitation.[27] The spectrum is dominated by transitions involving the symmetric stretch (ν_1) and bend (ν_2). Most interesting is the substantial intensity at 2190 cm^{-1} corresponding to the asymmetric-stretch overtone transition. The asymmetric-stretch coordinate is non-totally symmetric within the C_{2v} point group of ground-state OClO. For non-totally symmetric coordinates, fundamental resonance Raman intensity is not expected by symmetry, and this expectation is borne out by the very modest intensity at 1100 cm^{-1}. However, even-overtone transitions involving non-totally symmetric coordinates can demonstrate intensity if the curvature of the excited-state potential energy surface is different from that of the ground state.[28] The observation of asymmetric-stretch overtone intensity immediately demonstrates that the curvature of excited and ground states along this coordinate are significantly different. Recall that the observation of resonance Raman intensity indicates that evolution along the corresponding normal coordinate occurs following photoexcitation. Therefore, the pattern of intensities observed in Figure 2 demonstrates that, following photoexcitation of gaseous OClO, structural evolution occurs along all three normal coordinates, consistent with the conclusions reached through earlier analyses of the absorption spectrum as discussed above.

In contrast to the gas phase, the resonance Raman spectrum of OClO in solution demonstrates only modest intensity for transitions involving the asymmetric stretch. Figure 2 presents the resonance Raman spectrum of OClO dissolved in cyclohexane.[29,30] Significant intensity is observed for transitions involving the symmetric-stretch and bend coordinates, demonstrating that excited-state structural evolution occurs along these coordinates, similar to the evolution that occurs in the gas phase. However, the asymmetric-stretch overtone intensity is extremely modest. In studies of OClO dissolved in water or chloroform, essentially no intensity was observed for the asymmetric-stretch overtone transition.[31,32] The predicted intensity for this transition employing both the double-well and ab initio models was determined and shown to be substantially greater than that observed. This result demonstrates that neither gas-phase surface provides an accurate description of the excited-state potential energy surface along this coordinate in solution. Instead, the limited asymmetric-stretch overtone intensity was found to be consistent with a modest reduction in frequency from 1100 cm^{-1} in the ground state to ~850 cm^{-1} in the excited state. In other words, the substantial evolution that occurs along this coordinate in the gas phase is significantly reduced in solution. Furthermore, the absence of significant asymmetric-stretch overtone intensity in all solvents studied to date indicates that limited excited-state structural evolution along the asymmetric-stretch coordinate may be a common feature of OClO photochemistry in solution.

The Role of Symmetry in OClO Photochemistry. Through analysis of the gas- and solution-phase absorption and resonance Raman data, a detailed description of excited-state structural evolution that occurs following OClO photoexcitation has been developed.[27,29−32] A schematic depiction of this evolution is presented in Figure 3. In both the gas phase and solution, significant excited-state structural evolution occurs along the symmetric-stretch and bend coordinates. The evolution along the

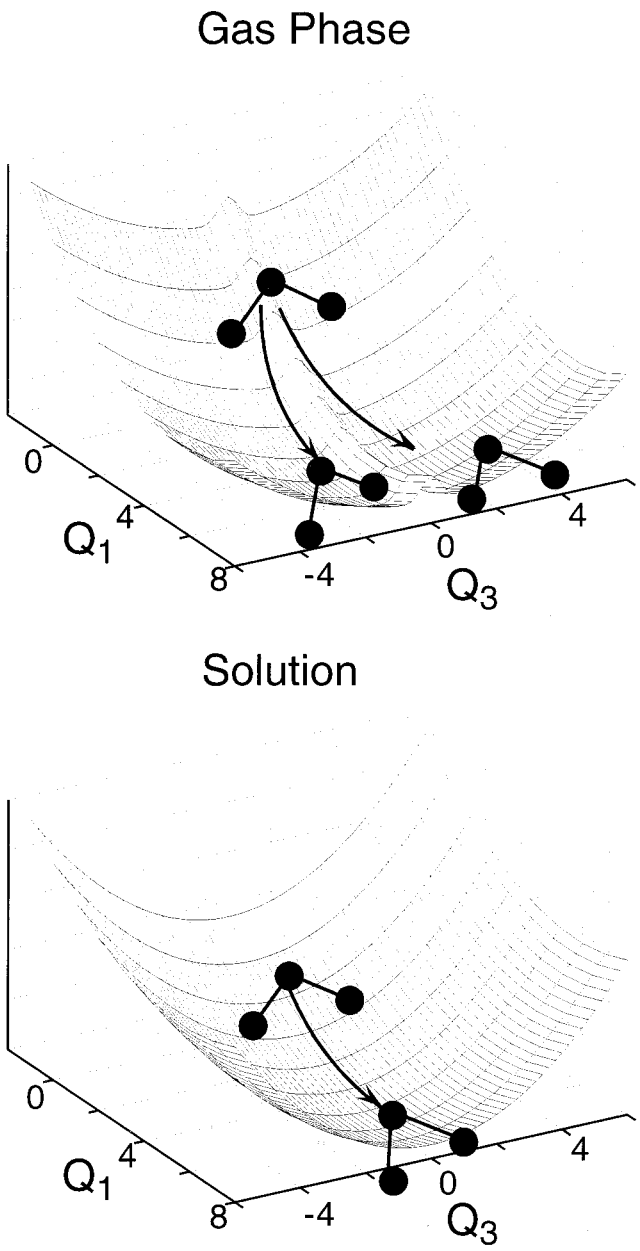

FIGURE 3. Depictions of the optically prepared $^2A_2$ surface along the symmetric- (Q_1) and asymmetric-stretch coordinates (Q_3) in dimensionless units. The gas-phase potential energy surface is that determined by Richard and Vaida.[18] The solution-phase surface is that determined by resonance Raman intensity analysis.[29,31] Notice the absence of evolution along the asymmetric-stretch coordinate in solution, resulting in the preservation of ground-state C_{2v} symmetry in the excited state.

symmetric stretch is depicted as motion along Q_1 in the figure, and motion along the bend has been suppressed for clarity. Inspection of the figure demonstrates that the major difference in structural evolution between the gas and solution phases involves the asymmetric stretch (Q_3). Specifically, the substantial evolution along this coordinate that occurs in the gas phase does not occur in solution. In the gas phase, evolution along the asymmetric stretch results in the reduction of molecular symmetry from C_{2v} to C_s. However, this limited evolution along the asymmetric stretch in solution results in the preservation of C_{2v} symmetry in the excited state. It should be noted that Figure 3 depicts the double-well model for the $^2A_2$ surface along the asymmetric stretch; however, a similar dynamical picture can be generated using the ab initio potential energy surfaces.[33]

We have proposed that the preservation of C_{2v} symmetry on the $^2A_2$ surface is partially responsible for the increase in Φ_{Cl} in solution relative to the value in the gas phase.[29] Previous gas-phase experimental and theoretical studies provide support for this hypothesis. Ab initio calculations have indicated that the reduction of symmetry from C_{2v} to C_s serves to reduce the energy barrier for ClO and O formation such that ClO bond dissociation becomes essentially barrierless.[22] As such, only for geometries at or near C_{2v} is the production of Cl and O_2 predicted to be appreciable. Experimentally, studies of product formation following the photolysis of gas-phase OClO has shown that the excitation of transitions involving the asymmetric stretch results in roughly a 10-fold reduction in Φ_{Cl} relative to excitation of transitions involving the symmetric stretch only.[10] That is, evolution along the asymmetric stretch serves to promote ClO bond dissociation in favor of Cl production. Our results suggest that a similar mechanism is responsible for enhanced Cl production in solution. The weak intensity for the asymmetric-stretch overtone transition in solution demonstrates that limited excited-state evolution occurs along this coordinate, resulting in the preservation of C_{2v} symmetry in the excited state, thereby enhancing Φ_{Cl}.

Our focus has been on the dynamics that occur on the $^2A_2$ surface; however, it is recognized that the lower energy $^2A_1$ and $^2B_2$ excited states also participate in photoproduct production. The sequence of events in OClO photochemistry is believed to be as follows.[9] Internal conversion from the optically prepared $^2A_2$ surface results in production of the $^2A_1$ state, with subsequent production of the lower-energy $^2B_2$ state occurring through $^2A_1$ state internal conversion. Studies of O_2 emission following photoexcitation of OClO in polar and nonpolar solvents have demonstrated that in polar solvents, the production of Cl is accompanied by the production of O_2 ($^3\Sigma_g^-$).[34] However, in nonpolar solvents, O_2 ($^1\Delta_g$) is predominantly formed. Under C_{2v} symmetry, only the $^2B_2$ state correlates with the Cl + O_2 ($^1\Delta_g$) channel. Therefore, the O_2 emission studies suggest that in nonpolar and polar solvents, Cl is derived from the $^2B_2$ and $^2A_1$ surfaces, respectively. Given the similarity of the $^2A_2$ surfaces in water and cyclohexane, the RRIA results taken in combination with the O_2 emission results demonstrate that partitioning between the Cl + O_2 channels occurs after decay of the $^2A_2$ surface. The above discussion assumes that C_{2v} symmetry is preserved along the reaction coordinate; however, a reduction in molecular symmetry on either the $^2A_1$ or $^2B_2$ surface would substantially alter this picture. For example, symmetry reduction could result in the production of the peroxy isomer, ClOO, which is expected to undergo facile decay into Cl and O_2. Therefore, information regarding the rates and quantum yields for photoproduct formation is neces-

sary to further refine our description of OClO photochemisty in solution.

OClO Photoproduct Formation Dynamics

To understand the environmental impact of halooxides, it is necessary to know which photochemical pathways are available, and how partitioning between these pathways is dependent on environment. Compared to the gas phase, Φ_{Cl} is substantially larger in condensed environments, as was first demonstrated by Simon and coworkers.[14] Using transient absorption studies with 100-ps resolution, it was established that 355-nm photoexcitation of aqueous OClO results in the production of atomic chlorine with $\Phi_{Cl} = 0.1$. The evolution in optical density observed in these studies was interpreted in terms of ClOO production and subsequent ground-state decomposition to Cl and O_2. Later transient absorption studies of aqueous OClO performed with femtosecond time resolution confirmed the value of Φ_{Cl}; however, the mechanism of Cl production and the dynamics responsible for the evolution in optical density were questioned.[35−39] In particular, it was suggested that since $\Phi_{Cl} = 0.1$, the production of ClO and O remained the dominant photochemical channel in solution. Consistent with this observation, the evolution in optical density was interpreted in terms of the production of ClO and O and the subsequent recombination of these photofragments to produce vibrationally excited OClO in the electronic ground state. Differentiation between these models awaited studies that could unequivocally determine the identity of those species formed following photoexcitation.

Geminate Recombination and OClO. We performed time-resolved resonance Raman studies of aqueous OClO to differentiate between the OClO photochemical models outlined above.[40,41] In this work, the evolution in the resonance Raman spectrum following excitation at 400 nm was monitored as a function of time utilizing a probe wavelength also at 400 nm. The evolution in Stokes scattering observed in this study is presented in Figure 4A. At 0-ps delay, when the pump and probe are overlapped in time, significant depletion in OClO scattering is observed. This observation is consistent with a reduction in the amount of ground-state OClO accompanying photoexcitation. As the temporal delay between the pump and probe increases, the OClO depletion intensity decreases up to 20 ps, after which time further evolution is not observed. The decay of OClO depletion intensity evident in Figure 4A provided direct confirmation of the geminate recombination model. In addition, the production of ClOO should be evidenced by scattering at 1442 cm^{-1}; however, essentially no intensity is observed in this frequency region. This result is consistent with the absence of ClOO, or with limited resonant enhancement of this species at this probe wavelength.

The kinetics associated with ground-state OClO production via geminate recombination were determined by plotting the depletion intensity for the symmetric-stretch fundamental transition (945 cm^{-1}) as a function of time

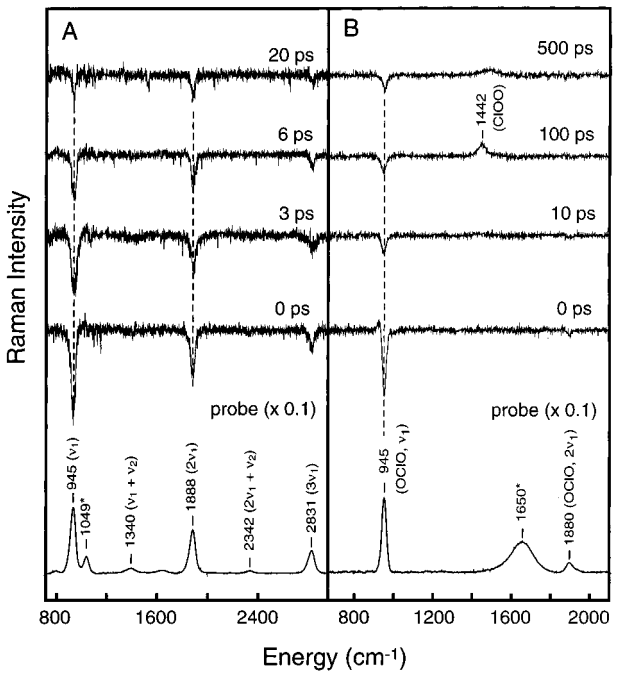

FIGURE 4. Time-resolved resonance Raman spectra of aqueous OClO. (A) Spectra obtained with degenerate pump and probe wavelengths of 400 nm. The spectrum on the bottom is that of the probe in the absence of photolysis, provided for comparison. The pump−probe delay for the various difference spectra is indicated. Note the depletion in OClO scattering intensity which recovers as the probe is delayed. This recovery demonstrates that the geminate recombination of the primary photofragments results in the reformation of OClO. (B) Spectra obtained with pump and probe wavelengths of 390 and 260 nm, respectively. In addition to the depletion and recovery in OClO scattering, intensity corresponding to ClOO is observed.

(Figure 5A). Inspection of these data reveals that the depletion recovery is biphasic, with roughly 30% of the recovery occurring by 1 ps. Consistent with this observation, the evolution in intensity was best modeled by a sum of two exponentials having time constants of 0.15 ps (i.e., significantly shorter than the instrument response) and ∼9 ps. A third, long-time component (10 000 ps, fixed) was also included in the model to reproduce the persistent depletion in scattering intensity at long delays. These time constants were interpreted as follows. Subpicosecond geminate recombination of the primary photofragments results in the production of vibrationally excited OClO, which undergoes intermolecular vibrational relaxation with a time constant of ∼9 ps. To further explore these assignments, time-resolved anti-Stokes experiments were performed.[41] The decay in anti-Stokes intensity was found to occur with a time constant of 9 ps, conclusively demonstrating that the slower time dynamics arise from vibrational relaxation. Finally, comparison of the early time depletion to that which persists at long delays established that 10% of photoexcited OClO goes on to form Cl, and to a minor extent solvent-separated ClO and O. The presence of geminate recombination was further confirmed by performing time-resolved resonance Raman studies in acetonitrile.[41] In this solvent, the absence of intermolecular hydrogen bonding provides for geminate

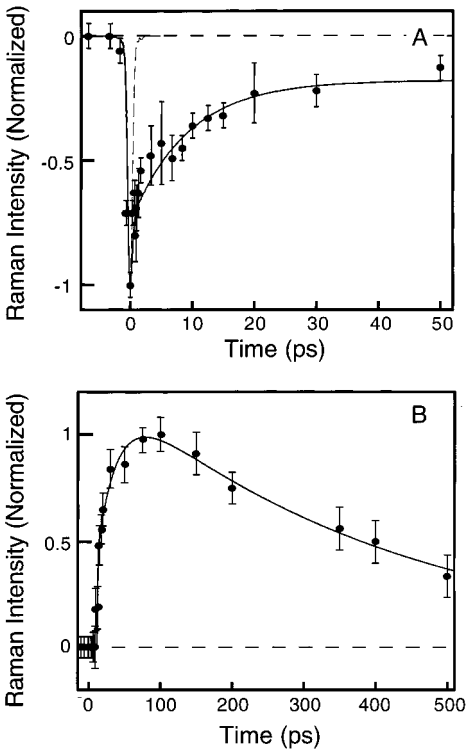

FIGURE 5. (A) OClO symmetric-stretch depletion intensity as a function of pump−probe delay. Intensities correspond to those measured at 400 nm. Best fit to the data by a sum of exponentials convolved with the instrument response (solid line) was obtained with time constants of 0.15 ± 0.1 ps, 33.0 ± 8.1 ps, and a long time component necessary to reproduce the long time offset in intensity. The instrument response is shown as the dashed line. (B) Intensity of the ClOO transition at 1442 cm^{-1} as a function of pump−probe delay. The data were best fit by a sum of two exponentials convolved with the instrument response (solid line), resulting in appearance and decay time constants of 27.9 ± 4.5 and 398 ± 50 ps, respectively.

recombination quantum yields that are typically reduced relative to those in water.[42] Consistent with this expectation, geminate recombination of ClO and O was found to be reduced by a factor of 5 in acetonitrile relative to that in water, conclusively demonstrating the importance of geminate recombination in describing the condensed-phase photochemistry of OClO.

Cl Production following OClO Photoexcitation. As described above, $\Phi_{Cl} = 0.1$ for aqueous OClO; however, the question remains as to the mechanism of Cl formation. The production of Cl is accompanied by the formation of molecular oxygen in either the electronic ground ($^3\Sigma_g^-$) or excited ($^1\Delta_g$) state. As outlined above, partitioning between these states is dependent on solvent polarity, suggesting that there are two pathways for Cl production.[34] To investigate the pathway involving ClOO formation and subsequent decomposition to form Cl and O_2 ($^3\Sigma_g^-$), we performed time-resolved resonance Raman studies in which the events initiated by 390-nm photoexcitation were monitored using a 260-nm probe (Figure 4B).[43] This probe wavelength was chosen since the absorption cross section of ClOO in ice is known to be substantial at this wavelength.[44] At 0 ps, depletion in OClO scattering is observed, with the extent of depletion decreasing as the pump−probe delay is increased. This result is entirely consistent with the results obtained at 400 nm. However, positive intensity is now evident at 1442 cm^{-1}, consistent with the formation of ClOO. The appearance of ClOO intensity is substantially delayed relative to zero delay, and decay of this intensity occurs out to the longest delays studied (500 ps), demonstrating that ClOO decomposes on the sub-nanosecond time scale.

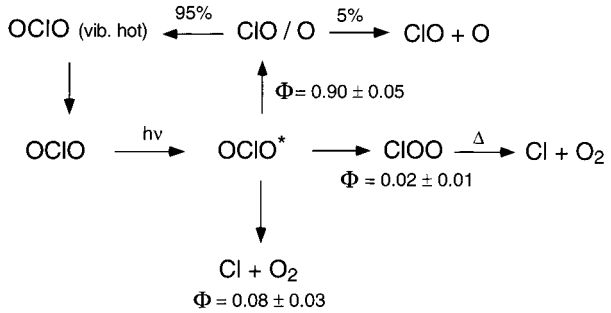

FIGURE 6. Current picture of aqueous OClO photochemistry. The quantum yields for various photochemical pathways are indicated.

The ClOO production and decay kinetics were determined by plotting the intensity of the 1442 cm^{-1} transition as a function of delay as presented in Figure 5B. These data were best modeled by a sum of two exponentials, resulting in appearance and decay time constants of ∼28 and ∼400 ps, respectively. Reproduction of the data necessitated an additional ∼13-ps delay relative to zero time to mimic the absence of intensity at early delays. The ClOO appearance time constant most likely represents a convolution of production and vibrational relaxation, and the long time decay component is assigned to thermal decomposition of ground-state ClOO, resulting in the production of Cl and O_2 ($^3\Sigma_g^-$). This assignment was recently verified by time-resolved absorption studies in which Cl production was observed on a corresponding time scale.[45] Most striking is that the production of ClOO occurs on a much longer time scale relative to the sub-picosecond re-formation of OClO. This difference suggests that ClOO is not produced by geminate recombination of the primary photofragments but is produced via OClO photoisomerization. Symmetry correlation diagrams demonstrate that the lowest-energy excited state of OClO correlates with the $^2A'$ excited state of ClOO and not the $^2A''$ ground state.[8] Internal conversion from the $^2A'$ surface on the picosecond time scale would explain the delayed appearance of ground-state ClOO relative to the rapid production of OClO via geminate recombination. An alternative mechanism supported by ab initio studies involves the initial production of excited-state ClOO followed by rapid dissociation, resulting in the production of Cl and O_2.[22] Recombination of these fragments could provide for the appearance of ClOO on the picosecond time scale.

The combined time-resolved resonance Raman and transient absorption studies of aqueous OClO have provided information regarding the rates and quantum yields for photoproduct formation, with current quantum yield values for photoexcitation at 400 nm presented in Figure 6. As discussed above, the quantum yield for dissociation

into ClO and O is 0.90, such that the dominant pathway following OClO photoexcitation is the production and subsequent geminate recombination of the ClO and O photofragments. The remainder of photoexcited OClO goes on to form Cl. The modest resonance Raman intensity observed for ClOO (Figure 4B) suggests that formation and decomposition of this species represents a minor Cl production channel. Consistent with this expectation, transient absorption studies have shown that the quantum yield for ClOO production is only 0.02.[45] This value, when taken in combination with the 0.10 quantum yield for overall Cl production, demonstrates that a second photochemical pathway leading to Cl formation is present. Indeed, transient absorption studies have shown that in addition to ClOO decomposition, Cl production occurs via decay of an intermediate that decomposes to form Cl with a time constant of ~6 ps.[36,37] The identity of this intermediate is not known at present, but it has been proposed that it is a highly distorted form of OClO.

Summary and Questions Unanswered

The resonance Raman studies presented here provide a detailed picture of OClO photochemistry in solution. In particular, the RRIA studies have shown that the photoinitiated excited-state structural relaxation is substantially different in solution relative to that in the gas phase. TRRR studies have shown that the presence of solvent leads to efficient recombination of the primary ClO and O photofragments, resulting in the production of ground-state OClO. These studies also demonstrated that ClOO is formed to a minor extent, with the thermal decomposition of this species providing for Cl production on the subnanosecond time scale.

Although a rather detailed description of OClO photoreactivity has been developed, there are many issues yet to be resolved. For example, the processes resulting in the early time production of Cl remain unclear, and a complete description of this process awaits the identification of the Cl precursor. Another unresolved issue involves the influence of actinic wavelength on Cl production. Gas-phase studies have shown that Φ_{Cl} is extremely dependent on actinic wavelength.[10] However, photochemical action spectra of OClO embedded in water clusters suggest that a similar dependence is lost in the presence of solvent.[46] Although femtosecond transient absorption studies have shown that the efficiency of geminate recombination is dependent on actinic wavelength,[47] a corresponding dependence regarding photoproduct quantum yields has not been demonstrated. Finally, it is unclear to what extent OClO reflects halooxide photoreactivity as a whole. This issue can be addressed only by performing studies of other halooxides.[48] It is hoped that through such comparative studies, the fundamental details underlying the phase-dependent photochemical reactivity of halooxides will be understood.

I would like to acknowledge the vital contributions of my coworkers, Bethany Barham, Anthony Esposito, Kate Foster, Sophia Hayes, Matthew Philpott, and Carsten Thomsen (Aarhus University, Denmark). The National Science Foundation is acknowledged for their support of this work (CHE-9701717 and CHE-0091320). Acknowledgment is also made to the donors of the Petroleum Research Fund, administered by the American Chemical Society. P.J.R. is the recipient of a Dreyfus New-Faculty Award, a Cottrell Fellowship of the Research Corporation, and an Alfred P. Sloan Fellowship.

References

(1) Wayne, R. P.; Poulet, G.; Biggs, P.; Burrows, J. P.; Cox, R. A.; Crutzen, P. J.; Hayman, G. D.; Jenkin, M. E.; Le Bras, G.; Moortgat, G. K.; Platt, U.; Schindler, R. N. Halogen Oxides: Radicals, Sources and Reservoirs in the Laboratory and in the Atmosphere. *Atmos. Environ.* **1995**, *29*, 2677−2881.
(2) Farman, J. C.; Gardiner, B. G.; Shanklin, J. D. Large Losses of Total Ozone in Antarctica Reveal Seasonal ClO_x/NO_x Interaction. *Nature* **1985**, *315*, 207−210.
(3) Molina, M. J.; Molina, L. T.; Golden, D. M. Environmental Chemistry (Gas and Gas−Solid Interactions): The Role of Physical Chemistry. *J. Phys. Chem.* **1996**, *100*, 12888−12896.
(4) Rowland, F. S. Stratospheric Ozone Depletion. *Annu. Rev. Phys. Chem.* **1991**, *42*, 731−768.
(5) Wayne, R. P. *The Chemistry of Atmospheres*, 2nd ed.; Oxford Science Publications: Oxford, 1991.
(6) Solomon, S.; Borrmann, S.; Garcia, R. R.; Portmann, R.; Thomason, L.; Poole, L. R.; Winker, D.; McCormick, M. P. Heterogeneous Chlorine Chemistry in The Tropopause Region. *J. Geophys. Res.* **1997**, *102*, 21411−21429.
(7) Solomon, S.; Garcia, R. R.; Rowland, F. S.; Wuebbles, D. J. On the Depletion of Antartic Ozone. *Nature* **1986**, *321*, 755−758.
(8) Vaida, V.; Simon, J. D. The Photoreactivity of Chlorine Dioxide. *Science* **1995**, *268*, 1443−1448.
(9) Vaida, V.; Solomon, S.; Richard, E. C.; Ruhl, E.; Jefferson, A. Photoisomerization of OClO: a Polar Ozone Depletion Mechanism? *Nature* **1989**, *342*, 405−408.
(10) Davis, H. F.; Lee, Y. T. Photodissociation Dynamics of OClO. *J. Chem. Phys.* **1996**, *105*, 8142−8163.
(11) Arkell, A.; Schwager, I. Matrix Infrared Study of the ClOO Radical. *J. Am. Chem. Soc.* **1967**, *89*, 5999−6006.
(12) Muller, H. S. P.; Willner, H. Vibrational and Electronic Spectra of Chlorine Dioxide, OClO and Chlorine Superoxide, ClOO, Isolated in Cryogenic Matrices. *J. Phys. Chem.* **1993**, *97*, 10589−10598.
(13) Pursell, C. J.; Conyers, J.; Alapat, P.; Parveen, R. Photochemistry of Chlorine Dioxide in Ice. *J. Phys. Chem.* **1995**, *99*, 10433−10437.
(14) Dunn, R. C.; Flanders, B. N.; Simon, J. D. Solvent Effects on the Spectroscopy and Ultrafast Photochemistry of Chlorine Dioxide. *J. Phys. Chem.* **1995**, *99*, 7360−7370.
(15) Graham, J. D.; Roberts J. T.; Brown, L.; Vaida, V. The Uptake of Chlorine Dioxide by Model Polar Stratospheric Cloud Surfaces: Ultrahigh Vacuum Studies. *J. Phys. Chem.* **1996**, *100*, 3115−3120.
(16) Brown, L. A.; Vaida, V.; Handson, J. D.; Graham, J. D.; Roberts, J. T. The Uptake of Chlorine Dioxide by Model PSCs under Stratospheric Conditions. *J. Phys. Chem.* **1996**, *100*, 3121−3125.
(17) Coon, J. B. Vibrational Analysis of the Chlorine Dioxide Absorption Spectrum. *Phys. Rev.* **1940**, *58*, 926−927.
(18) Richard, E. C.; Vaida, V. The Direct Near Ultraviolet Adsorption Spectrum of the $A^2A_2-X^2B_1$ Transition of Jet-Cooled Chlorine Dioxide. *J. Chem. Phys.* **1991**, *94*, 153−162.
(19) Richard, E. C.; Vaida, V. The Photochemical Dynamics of the $^2A_2$ State of Chlorine Dioxide. *J. Chem. Phys.* **1991**, *94*, 163−171.
(20) Brand, J. C. D.; Redding, R. W.; Richardson, A. W. The 4750-Å Band System of Chlorine Dioxide. Rotational Analysis, Force Field and Intensity Calculations. *J. Mol. Spectrosc.* **1970**, *34*, 399−414.
(21) Peterson, K. A. Accurate ab initio Near-Equilibrium Potential Energy and Dipole Moment Functions of the X $^2B_1$ and First Excited $^2A_1$ Electronic States of OClO and OBrO. *J. Chem. Phys.* **1998**, *109*, 8864−8875.
(22) Peterson, K. A.; Werner, H. J. The Photodissociation of ClO_2-Potential Energy Surfaces. *J. Chem. Phys.* **1996**, *105*, 9823−9832.
(23) Myers, A. B. 'Time-Dependent' Resonance Raman Theory. *J. Raman Spectrosc.* **1997**, *28*, 389−401.
(24) Myers, A. B.; Mathies, R. A. In *Biological Applications of Raman Spectroscopy*, *Vol. 2*, *Resonance Raman Spectra of Polyenes and Aromatics*; Spiro, T. G., Ed.; John Wiley & Sons: New York, 1987; Vol. 2, pp 1−58.
(25) Lee, S.-Y.; Heller, E. J. Time-Dependent Theory of Raman Scattering. *J. Chem. Phys.* **1979**, *71*, 4777−4788.
(26) Tannor, D. J.; Heller, E. J. Polyatomic Raman Scattering for General Harmonic Potentials. *J. Chem. Phys.* **1982**, *77*, 202−218.

(27) Esposito, A. P.; Stedl, T.; Jonsson, H.; Reid, P. J.; Peterson, K. A. An Absorption and Resonance Raman Study of Chlorine Dioxide in the Gas Phase. *J. Phys. Chem. A* **1999**, *103*, 1748−1757.
(28) Lawless, M. K.; Reid, P. J.; Mathies, R. A. In *Ultrafast Dynamics of Chemical Systems*; Simon, J. D., Ed.; Kluwer: Amsterdam, 1994; pp 267−287.
(29) Esposito, A.; Foster, C.; Beckman, R.; Reid, P. J. Resonance Raman Intensity Analysis of Chlorine Dioxide. *J. Phys. Chem. A* **1997**, *101*, 5309−5319.
(30) Reid, P. J.; Esposito, A. P.; Foster, C. E.; Beckman, R. A. Evidence for the $^2B_1-^2A_1$ Electronic Transition in Chlorine Dioxide from Resonance Raman Depolarization Ratios. *J. Chem. Phys.* **1997**, *107*, 8262−8274.
(31) Foster, C. E.; Reid, P. J. The Excited-State Reaction Dynamics of Chlorine Dioxide in Water from Absolute Resonance Raman Intensities. *J. Phys. Chem. A* **1998**, *102*, 3541−3549.
(32) Foster, C. E.; Barham, B. P.; Reid, P. J. Resonance Raman Intensity Analysis of Chlorine Dioxide Dissolved in Chloroform: the Role of Nonpolar Solvation. *J. Chem. Phys.* **2001**, *114*, 8492−8504.
(33) Xie, D.; Guo, H. A Refined Near-Equilibrium Potential Energy Surface and The Absorption Spectrum of OClO A($^2A_2$). *Chem. Phys. Lett.* **1999**, *307*, 109−116.
(34) Dunn, R. C.; Anderson, J. L.; Foote, C. S.; Simon, J. D. Solution Photochemistry of Chlorine Dioxide: Mechanisms for the Generation of Atomic Chlorine. *J. Am. Chem. Soc.* **1993**, *115*, 5307.
(35) Chang, Y. J.; Simon, J. D. Ultrafast Dynamics of Chlorine Dioxide Photochemistry in Water Studied by Femtosecond Transient Absorption Spectroscopy. *J. Phys. Chem.* **1996**, *100*, 6406−6411.
(36) Thøgersen, J.; Jepsen, P. U.; Thomsen, C. L.; Poulsen, J. A.; Byberg, J. R.; Keiding, S. R. Femtosecond Photolysis of ClO_2 in Aqueous Solution. *J. Phys. Chem.* **1997**, *101*, 3317−3323.
(37) Poulsen, J. A.; Thomsen, C. L.; Keiding, S. R.; Thøgersen, J. Vibrational Relaxation of ClO_2 in Water *J. Chem. Phys.* **1998**, *108*, 8461−8471.
(38) Philpott, M. J.; Charalambous, S.; Reid, P. J. Comparison of Chlorine Dioxide Photochemistry in Acetonitrile and Water using Subpicosecond Pump−Probe Spectroscopy *Chem. Phys. Lett.* **1997**, *281*, 1−9.
(39) Philpott, M. J.; Charalambous, S.; Reid, P. J. Ultrafast Pump−Probe Studies of Chlorine Dioxide Photochemistry in Water and Acetonitrile. *Chem. Phys.* **1998**, *236*, 207−224.
(40) Hayes, S. C.; Philpott, M. J.; Reid, P. J. The Dynamics of Photoproduct Formation of Aqueous Chlorine Dioxide: A Time-Resolved Resonance Raman Study. *J. Chem. Phys.* **1998**, *109*, 2596−2599.
(41) Hayes, S. C.; Philpott, M. P.; Mayer, S. G.; Reid, P. J. A Time-Resolved Resonance Raman Study of Chlorine Dioxide Photochemistry in Water and Acetonitrile. *J. Phys. Chem. A* **1999**, *103*, 5534−5546.
(42) Walhout, P. K.; Alfano, J. C.; Thakur, K. A. M.; Barbara, P. F. Ultrafast Experiments on the Photodissociation, Recombination, and Vibrational Relaxation of I_2^-: Role of Solvent-Induced Solute Charge Flow. *J. Phys. Chem.* **1995**, *99*, 7568−7580.
(43) Thomsen, C. L.; Philpott, M. P.; Hayes, S. C.; Reid, P. J. Production of ClOO following the Photoexcitation of Aqueous OClO Studied by Two-color, Time-Resolved Resonance Raman Spectroscopy. *J. Chem. Phys.* **2000**, *112*, 505−508.
(44) Mauldin, R. L., III; Burkholder, J. B.; Ravishankara, A. R. A Photochemical, Thermodynamic, and Kinetic Study of ClOO. *J. Phys. Chem.* **1992**, *96*, 2582−2588.
(45) Thomsen, C. L.; Reid, P. J.; Keiding, S. R. The Quantum Yield for ClOO Formation Following Photolysis of Aqueous OClO Investigated by Femtosecond Transient Absorption Spectroscopy. *J. Am. Chem. Soc.* **2000**, *122*, 12795−12801.
(46) Kreher, C. J.; Carter, R. T.; Huber, J. R. Photodissociation of OClO and Ar/OClO and H_2O/OClO Clusters Studied by the Resonance Enhanced Multiphoton Ionization-Time of Flight Method. *J. Chem. Phys.* **1999**, *110*, 3309−3319.
(47) Thøgersen, J.; Thomsen, C. L.; Poulsen, J. Aa.; Keiding, S. R. Chemical Reactions in Liquids: Photolysis of OClO in Water. *J. Phys. Chem. A* **1998**, *102*, 4186−4191.
(48) Esposito, A. P.; Reid, P. J.; Rousslang, K. W. A Resonance Raman Study of Cl_2O Photochemistry in Solution: Evidence for ClClO Formation. *J. Photochem. Photobiol. A, Chemistry* **1999**, *129*, 9−15.

AR010064U